J Mater Sci (2008) 43:3153–3161
DOI 10.1007/s10853-008-2499-z

Cerium ion redox system in CeO_2–xFe_2O_3 solid solution at high temperatures (1,273–1,673 K) in the two-step water-splitting reaction for solar H_2 generation

H. Kaneko · H. Ishihara · S. Taku · Y. Naganuma · N. Hasegawa · Y. Tamaura

Received: 27 November 2007 / Accepted: 24 January 2008 / Published online: 28 February 2008

Abstract CeO_2–xFe_2O_3 ($x = 0.026$–0.214) solid solutions with different Ce:Fe mole ratios (Ce:Fe = 9.5:0.5–7.0:3.0) were prepared as reactive ceramics with the combustion method for solar hydrogen production. The prepared CeO_2–xFe_2O_3 solid solutions were characterized by X-ray diffractometry, ICP atomic emission spectrometry, and Mössbauer spectroscopy. Two-step water-splitting reaction with the CeO_2–xFe_2O_3 solid solution proceeded at 1,673 K for the O_2-releasing reaction and at 1,273 K for the H_2-generation reaction by irradiation of an infrared imaging lamp as a solar simulator. The amounts of H_2 gas evolved in the H_2-generation reaction with CeO_2–xFe_2O_3 solid solutions were 0.97–1.8 cm^3/g, the evolved H_2/O_2 ratio was approximately equal to 2 of the stoichiometric value. The amounts of H_2 and O_2 gases were independent of the Ce:Fe mole ratio in the CeO_2–xFe_2O_3 solid solution. It was suggested that the O_2-releasing and H_2-generation reactions with the CeO_2–xFe_2O_3 solid solution were repeated with the reduction and oxidation of Ce^{4+}–Ce^{3+} enhanced by the presence of Fe^{3+}–Fe^{2+}.

Introduction

Hydrogen production with concentrated solar thermal energy using a two-step water-splitting reaction has been proposed in the field of solar chemistry [1]. Various redox systems of reactive ceramic (MO) have been studied for two-step water-splitting reaction [2]. They can be represented as:

Oxygen-releasing step
$$MO_{ox} + \text{thermal energy} = MO_{red} + 1/2O_2(g) \tag{1}$$

Hydrogen-generation step
$$MO_{red} + H_2O(g) = MO_{ox} + H_2(g) \tag{2}$$

where MO_{ox} and MO_{red} denote the oxidized and reduced states of a metal oxide, respectively. Hydrogen and oxygen are obtained by repeating two steps alternately in the two-step water-splitting cycle. Iron-based oxides (mainly ferrites) have been widely investigated for the reactive ceramic applied to the two-step water-splitting reaction [2]. Many of ferrite compounds melt and sinter in the O_2-releasing reaction at a high temperature, since the appropriate O_2-releasing temperatures are close to their melting points. Recently, a reactive ceramic of the cerium oxide system has been studied for the two-step water-splitting reaction with concentrated solar thermal energy such as CeO_2 or CeO_2- transition metal oxide solid solution because of the stability at a high temperature for the O_2-releasing reaction [3, 4].

The formation of a solid solution between MO_x (M = Mn, Fe, or Ni) and CeO_2 has been found to be effective for the enhancement of the ability for the O_2-releasing reaction at lower temperatures compared with CeO_2 [4]. The valence of cerium ion (Ce^{4+}–Ce^{3+}) in ceria changes from +4 to +3 without phase transition of the fluorite structure in spite of the increase in ionic radii (Ce^{3+}:0.1143 nm > Ce^{4+}:0.097 nm) [5]. The cyclic two-step water-splitting reaction with a CeO_2-based solid solution was repeated, and the thermal stability of the CeO_2-based solid solution was confirmed. Furthermore,

---

H. Kaneko · H. Ishihara · S. Taku · Y. Naganuma ·
N. Hasegawa · Y. Tamaura (✉)
Research Center for Carbon Recycling and Energy,
Tokyo Institute of Technology, Ookayama 2-12-1, Meguro-ku,
Tokyo 152-8552, Japan
e-mail: ytamaura@chem.titech.ac.jp

CeO_2-based solid solutions have been investigated in other fields, including as a sensor for automobile exhaust gas emission control, as an electrolyte for solid oxide fuel cell, and as catalysts for oxidation and hydrogenation reactions [6, 7]. CeO_2–CuO solid solutions have been examined for selective oxidation of CO and oxidative steam reforming of methane [8–11]. A CeO_2–Fe_2O_3 solid solution was prepared for the synthesis of 3-pentanone from 1-propanol [12]. At a low-temperature nanoscale the CeO_2–Fe_2O_3 solid solution was synthesized with a high Fe^{3+} content [13]. The mechanism of the catalytic reaction with the CeO_2-based solid solution was revealed by Raman spectroscopy, X-ray absorption fine structure (XAFS), X-ray photoelectron spectroscopy (XPS), electron paramagnetic resonance (EPR), and Mössbauer spectroscopy at temperatures below 1,273 K in previous studies [6, 8–11, 14, 15].

The characteristics of ceria (CeO_2) are summarized by Trovarelli; it is noteworthy that ceria store and release oxygen, and form surface and bulk vacancies [6]. CeO_2-based mixed oxides and solid solutions are used in catalysts because of their high activities for the catalytic reaction and their high ionic conductivities. The remarkable features of the CeO_2-based catalyst depend on the effect of precious metal-ceria interactions and the activity of the redox couple Ce^{4+}–Ce^{3+} [6]. It is expected that a CeO_2-based solid solution enhances the activity of the two-step water-splitting reaction because of the metal-ceria interaction effect even at high temperatures and produces a large amount of hydrogen in the H_2-generation reaction.

The objectives of the present paper are to synthesize CeO_2–iron oxide solid solution (CeO_2–xFe_2O_3) with the fluorite structure in different mole ratios of Ce:Fe and to elucidate the mechanism of the two-step water-splitting reaction through the investigation of O_2-releasing and H_2-generation reactions with CeO_2–xFe_2O_3 at the high temperatures of 1,673 K and 1,273 K, respectively. The cyclic two-step water-splitting reaction with CeO_2–xFe_2O_3 is examined and the solid products after the reaction are characterized by X-ray diffractometry (XRD) and Mössbauer spectroscopy. Here we also report the H_2-generation reaction rate of CeO_2–xFe_2O_3 compared to that of Ni-ferrite ($NiFe_2O_4$) to confirm the prominent reactive ceramic for the practical solar hydrogen production. In other words, CeO_2–xFe_2O_3 is studied to obtain the suitable reactive ceramic for the developing rotary-type solar reactor [16].

Experimental

Synthesis of CeO_2–xFe_2O_3

All the chemicals used in the synthesis of CeO_2–xFe_2O_3 ($x = 0.026$, 0.038, 0.062, 0.088, 0.125, and 0.214, i.e., Ce:Fe = 9.5:0.5, 9.3:0.7, 8.9:1.1, 8.5:1.5, 8.0:2.0, and 7.0:3.0) via combustion method were of analytical grade. CeO_2–xFe_2O_3 was prepared as follows [8]: Cerium nitrate hexahydrate ($Ce(NO_3)_3 \cdot 6H_2O$), iron nitrate enneahydrate ($Fe(NO_3)_3 \cdot 9H_2O$), and urea ($CO(NH_2)_2$) were mixed with a Ce:Fe mole ratio of 9.5:0.5–7:3 in a minimum volume of demineralized water to obtain a transparent solution. The initial urea/nitrate mole ratio was adjusted in 4.2 according to the optimum urea/nitrate mole ratio for the oxidation of CO [8]. The mixed solutions were heated for about 15 min at 343 K and the resulting adhesive solution with high viscosity was introduced in an open muffle furnace, which was preheated at 723 K, with a disposable aluminum tray. The adhesive solution started boiling with frothing and foaming in 10 min; then in a few minutes the foam ignited spontaneously with vigorous evolution of gases, yielding foamy, voluminous lumps. The porous lumps obtained after combustion were ground in an agate mortar to gain the powdered product. The powdered product contains small amounts of carbon residues, because combustion by spontaneous ignition lasts only for about 10 s. To burn up carbon residues, the powders were further heated in the electric furnace at 823 K for 2 h in air atmosphere.

The product was identified by XRD with Ni-filtered Cu-Kα radiation (Rigaku, RINT ultima$^+$), and the lattice constant a_0 of the product was calculated using the JADE ver.5.0 (Rigaku) software program. The products calcined at 823 K were dissolved in 36 M solution of H_2SO_4 and 30% solution of H_2O_2, then the mole ratios of Ce and Fe in the products were determined by the inductively coupled plasma atomic emission spectrometer (ICP-AES, Thermo Jarrell Ash IRIS/AP). Mössbauer spectra of the products were measured with ^{57}Co source diffused in metallic Rh and calibrated with an iron foil absorber at a room temperature. The spectra were analyzed by computer fitting to a Lorentzian curve, and the hyperfine parameters were calculated using IGOR Pro Ver.5.0 (WaveMetrics, Inc.) and WinNormos-for-Igor (Wissenschaftliche Elektronik GmbH) software programs.

O_2-releasing and H_2-generation reactions

Powdered CeO_2–xFe_2O_3 (Ce:Fe = 9.5:0.5–7:3) sample calcined at 823 K (0.4 g) was packed in the quartz tubular reactor (5–18 mm i.d. × 490 mm long) shown in Fig. 1. The CeO_2–xFe_2O_3 was mounted on a platinum mesh vessel with a Pt–Pt/Rh thermocouple sensor. For the O_2-releasing reaction experiment, the sample was reacted in a quartz tubular reactor under an Ar gas flow (100 cm^3/min) at 1,673 K by heating with the infrared imaging lamps (ULVAC-RIKO, Inc., VHT–44E). Irradiation from the infrared imaging lamps was regulated by the temperature program controller (ULVAC-RIKO, Inc., TPC-1000) to obtain a

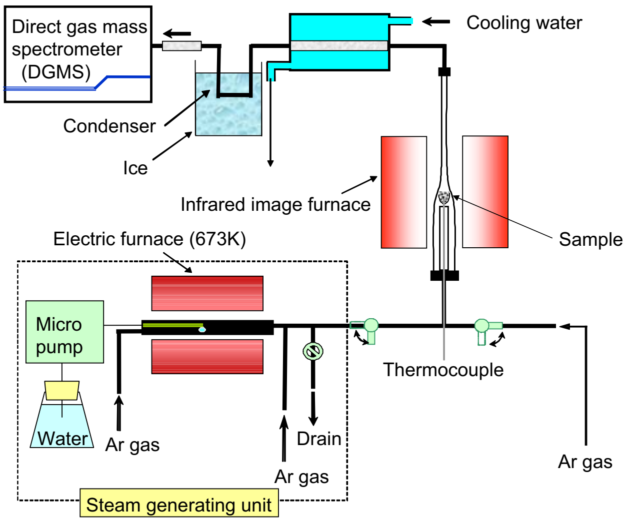

Fig. 1 Experimental set-up for O_2-releasing and H_2-generation reactions

definite reaction temperature, and the temperature was raised at the rate of 200 K/min. For the H_2-generation reaction experiment followed by the O_2-releasing reaction, steam was generated by dropping demineralized water with a micropump (0.020 mol/min) in an electric furnace at 673 K, and steam was passed through the reactor at a flow rate of 0.020 mol/min with an Ar gas (100 cm^3/min) as a carrier gas to react with the sample. The passage for steam to the reaction cell was all heated to ca. 400 K. The reaction temperature was lowered to 1,273 K at the rate of 200 K/min. The gaseous products in the O_2-releasing and the H_2-generation reactions were measured by direct gas mass spectrometer (VG Gas Analysis Systems, THERMOLAB). The O_2-releasing reaction and H_2-generation reaction were repeated alternately (the cyclic two-step water-splitting reaction). The solid product after O_2-releasing or H_2-generation reaction was identified by XRD and Mössbauer spectroscopy; then the lattice constant or the hyperfine parameters of the solid product was calculated.

H_2-generation reaction rate

The H_2-generation reaction rates of $CeO_2–xFe_2O_3$ and Ni-ferrite were evaluated for the H_2-generation reaction at 1,273 K. The H_2-generation reaction rate of $CeO_2–xFe_2O_3$ is the 90% amount of H_2 gas evolved in the H_2-generation reaction per g of the sample divided by the reaction time for 90% amount of H_2 gas. The two-step water-splitting reaction with Ni-ferrite was carried out at 1,773 K for the O_2-releasing reaction (5 min) and at 1,273 K for the H_2-generation reaction (8 min) using the same experimental set-up as for the $CeO_2–xFe_2O_3$. The Ni-ferrite used in the two-step water-splitting reaction was supplied by Soekawa Chemical Co. Ltd. (Japan). The H_2-generation reaction rate of Ni-ferrite is the 90% amount of H_2 gas evolved in the H_2-generation reaction per g of the sample divided by the reaction time for 90% amount of H_2 gas.

Results and discussion

Synthesis of $CeO_2–xFe_2O_3$

The samples of $CeO_2–xFe_2O_3$ (Ce:Fe = 9.5:0.5–7:3) prepared by calcination at 823 K were brown granules. The mole fractions of Ce and Fe in the samples are determined by ICP-AES, and the chemical compositions of the samples are summarized in Table 1. The chemical compositions of the samples prepared with the various mole ratios of Ce:Fe were close to those of the initial mixed solutions. Since $Ce(NO_3)_3 \cdot 6H_2O$ was so hygroscopic that it took up water during storage and weighing, the Ce content in the prepared samples was lower than that in the initial mixed solutions.

The XRD patterns of the $CeO_2–xFe_2O_3$ with Ce:Fe = 9.5:0.5–7.0:3.0 obtained by calcining at 823 K for 2 h are shown in Fig. 2a–f, respectively. The single-phase patterns with fluorite structure were observed for the products prepared with lower Fe content than Ce:Fe ratio of 8.0:2.0 (Fig. 2a–e). As can be seen from XRD pattern of (f) in Fig. 2, the peaks ascribed to the spinel structure appeared with the peaks of the fluorite structure in the sample of $CeO_2–xFe_2O_3$ with Ce:Fe = 7.0:3.0. The intensities of the diffraction lines assigned to the fluorite structure were almost equal for all $CeO_2–xFe_2O_3$ with different Ce:Fe ratios. The solid solutions between CeO_2 and Fe_2O_3 were formed in the preparation via the urea- nitrate combustion method in the range of Ce:Fe = 9.5:0.5–8.0:2.0.

The lattice constants (a_0) of $CeO_2–xFe_2O_3$ (Ce:Fe = 9.5:0.5–7.0:3.0) obtained by calcining at 823 K are listed in Table 2 with their standard deviations. The lattice constants of $CeO_2–xFe_2O_3$ with different Ce:Fe ratios

Table 1 Chemical composition of $CeO_2–xFe_2O_3$

Ce:Fe ratio in mixed solution for the preparation	Ce:Fe ratio in the prepared sample	Chemical formula
9.5:0.5	9.4:0.64	$Ce_{0.94}Fe_{0.06}O_{2-\alpha}$
9.3:0.7	9.1:0.93	$Ce_{0.91}Fe_{0.09}O_{2-\alpha}$
8.9:1.1	8.7:1.3	$Ce_{0.87}Fe_{0.13}O_{2-\alpha}$
8.5:1.5	8.1:1.9	$Ce_{0.81}Fe_{0.19}O_{2-\alpha}$
8.0:2.0	7.4:2.6	$Ce_{0.74}Fe_{0.26}O_{2-\alpha}$
7.0:3.0	4.2:5.8	Solid solution + spinel

Fig. 2 XRD patterns of the CeO_2–xFe_2O_3 with Ce:Fe ratio in a mixed solution for the preparation of (**a**) 9.5:0.5, (**b**) 9.3:0.7, (**c**) 8.9:1.1, (**d**) 8.5:1.5, (**e**) 8.0:2.0, and (**f**) 7.0:3.0 obtained by calcining at 823 K for 2 h

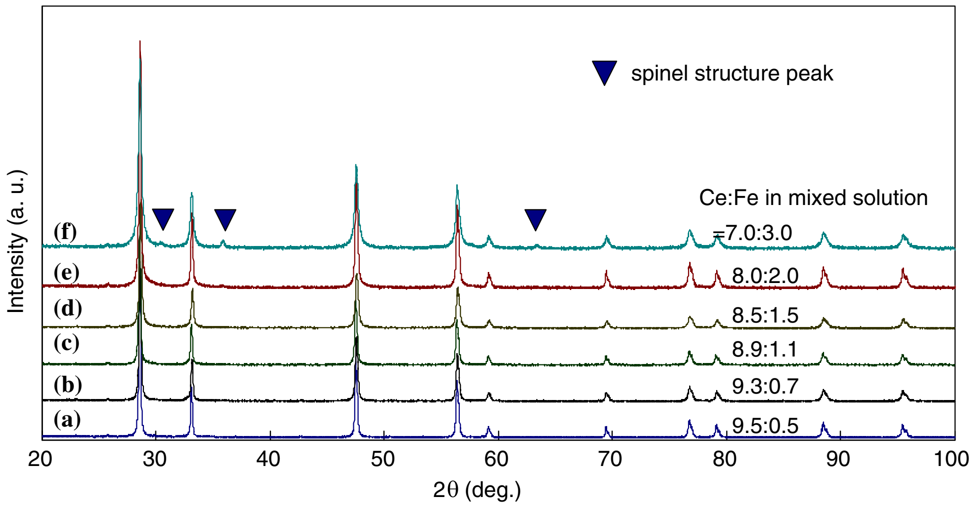

Table 2 Lattice constant of CeO_2–xFe_2O_3 calcined at 823 K

Ce:Fe ratio in CeO_2–xFe_2O_3	Calcined at 823 K (nm)	Standard deviation (nm)
9.5:0.5	0.54106	0.000010
9.3:0.7	0.54095	0.000017
8.9:1.1	0.54114	0.000017
8.5:1.5	0.54101	0.000035
8.0:2.0	0.54094	0.000009
7.0:3.0	0.54096	0.000027

(0.54094–0.54114 nm) were approximately equal for the fluorite structure pattern. The lattice constants of CeO_2–xFe_2O_3 (Ce:Fe = 9.5:0.5–7.0:3.0) calcined at 823 K were larger than those of CeO_2 (0.54093 nm) [4]. Since the chemical formula of CeO_2–xFe_2O_3 is represented as $Ce_aFe_bO_{2-\alpha}$ which is the oxygen-deficient structure, cation repulsion in CeO_2–xFe_2O_3 with the fluorite structure is larger than that in CeO_2.

Mössbauer spectra of the CeO_2–xFe_2O_3 with Ce:Fe = 9.5:0.5, 9.3:0.7, 8.9:1.1, 8.0:2.0, and 7.0:3.0 obtained by calcining at 823 K for 2 h are shown in Fig. 3a–e, respectively. Their best-fit hyperfine parameters (isomer shift, quadrupole splitting, and hyperfine magnetic field) are summarized in Table 3. The Mössbauer spectra for the CeO_2–xFe_2O_3 with Ce:Fe = 9.5:0.5, 9.25:0.75, and 8.9:1.1 were fitted with a doublet (Fig. 3a–c). The values of the isomer shift (mm/s) for the samples indicate that the iron is predominantly Fe^{3+} and in octahedral coordination [17]. The Mössbauer hyperfine parameters (isomer shift: 0.35 mm/s and quadrupole splitting: 0.98 mm/s) are typical of Fe^{3+} ions in the high-spin state in γ-Fe_2O_3 [14], and similar to those of the high-spin Fe^{3+} ions with a distorted octahedral coordination in a ceria-like solid solution ($Ce_{1-x}Fe_xO_2$) [13, 18, 19]. The relatively wide sextet signals appeared with a doublet signal in the spectrum of the CeO_2–xFe_2O_3 with Ce:Fe = 8.0:2.0 (Fig. 3d). The spectrum of the CeO_2–xFe_2O_3 with Ce:Fe = 7.0:3.0 (Fig. 3e) consists of a doublet and a sextet. The sextet signals with an isomer shift of 0.33 mm/s and a hyperfine magnetic field of 49 T are nearly equal to the magnetic static material of γ-Fe_2O_3 [20]. Because the fluorite structure and spinel structure were observed in the XRD pattern for the CeO_2–xFe_2O_3 with Ce:Fe = 7.0:3.0, a doublet and a sextet of Mössbauer spectroscopy arise from the octahedral-coordinated Fe^{3+} in a substitutional solid solution of CeO_2 and the γ-Fe_2O_3 phase, respectively.

O_2-releasing and H_2-generation reactions

The relationship between the amounts of H_2 and O_2 gases evolved in the two-step water-splitting reaction and the mole ratio of Ce:Fe in the mixed solution for preparation are demonstrated in Fig. 4. The average volume of the evolved H_2 and O_2 gases were calculated for four runs of the cyclic two-step water-splitting reaction. The amounts of H_2 and O_2 gases fluctuated between 1.0 cm^3/g and 1.8 cm^3/g and between 0.6 cm^3/g and 1.1 cm^3/g, respectively, with regard to the mole ratio of Ce:Fe in the CeO_2–xFe_2O_3 solid solution. It can be presumed that the fluctuations in the evolutions of H_2 and O_2 gases are due to the difference in characteristics of the solid solution particles caused by the vigorous combustion in the preparation. Since the amounts of H_2 and O_2 gases were independent of the mole ratio of Ce:Fe, it was suggested that the O_2-releasing and H_2-generation reactions with the CeO_2–xFe_2O_3 solid solution were repeated without the redox reaction of Fe^{3+}–Fe^{2+} but with the redox reaction of Ce^{4+}–Ce^{3+}. The average mole ratios of H_2/O_2 evolved in the two-step water-splitting reaction with CeO_2–xFe_2O_3 with different Ce:Fe ratios were 1.8, 1.6, 1.6, 1.9, 1.8, and 1.5 for Ce:Fe = 9.5:0.5, 9.3:0.7,

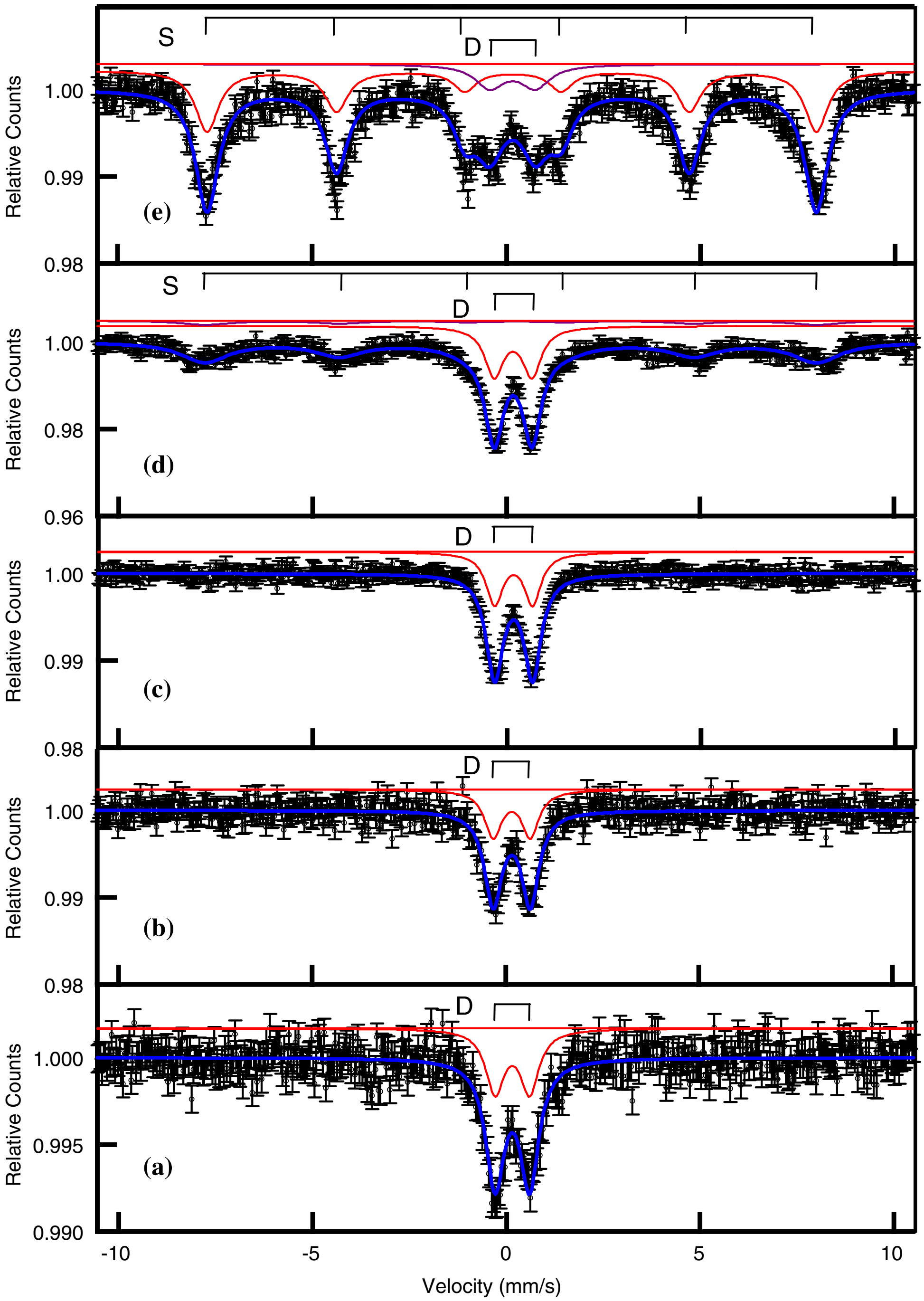

Fig. 3 Mössbauer spectra of the CeO_2–xFe_2O_3 with Ce:Fe ratio in a mixed solution for the preparation of (**a**) 9.3:0.7, (**b**) 8.9:1.1, (**c**) 8.5:1.5, (**d**) 8.0:2.0, and (**e**) 7.0:3.0 obtained by calcining at 823 K for 2 h. D: doublet, S: sextet

8.9:1.1, 8.5:1.5, 8.0:2.0, and 7.0:3.0, respectively. Since the ideal mole ratio of H_2/O_2 equals 2 in the stoichiometric two-step water-splitting reaction and the average mole ratios of H_2/O_2 were nearly equal to 2 for CeO_2–xFe_2O_3 systems, the two-step water-splitting reaction with CeO_2–xFe_2O_3 was found to proceed stoichiometrically.

Figure 5b and c show the profiles of O_2 and H_2 evolutions in the cyclic two-step water-splitting (O_2-releasing and H_2-generation) reaction repeated 11 runs using CeO_2–xFe_2O_3 with Ce:Fe = 8.9:1.1, respectively. The temperature of the sample regulated by a program controller was demonstrated in Fig. 5a. The appearance of the large peak of the O_2 evolution in the first O_2-releasing reaction agreed with the previous study [4]. The peak of the O_2 evolution observed in the 1st O_2-releasing reaction at 1,673 K was slightly larger (1.6 cm^3/g) than that in the subsequent O_2-releasing reactions (1.3 cm^3/g). The reason for the excess O_2 evolution in the 1st O_2-releasing reaction is discussed in the following Mössbauer spectroscopy study. Large noise in O_2-releasing profile was observed at

Table 3 Mössbauer spectroscopy parameters for prepared CeO_2–xFe_2O_3 with different Ce:Fe ratio

Ce:Fe in CeO_2–xFe_2O_3		Isomer shift (mm/s)	Quadrupole splitting (mm/s)	Hyperfine magnetic field (T)
9.5:0.5	D	0.33	0.89	
9.3:0.7	D	0.34	0.96	
8.9:1.1	D	0.35	0.98	
8.0:2.0	D	0.35	0.98	
	S	0.36	−0.15	48.9
7.0:3.0	D	0.34	1.17	
	S	0.33	−0.03	48.6

D = doublet; S = sextet

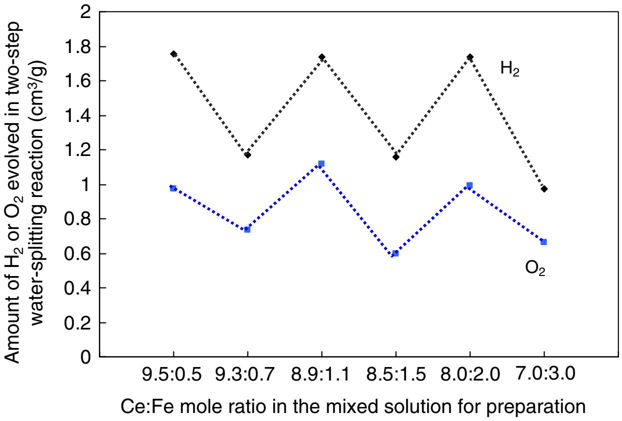

Fig. 4 Relationship between the amount of H_2/O_2 evolved in the two-step water-splitting reaction and Ce:Fe mole ratio in the mixed solution for the preparation of CeO_2–xFe_2O_3

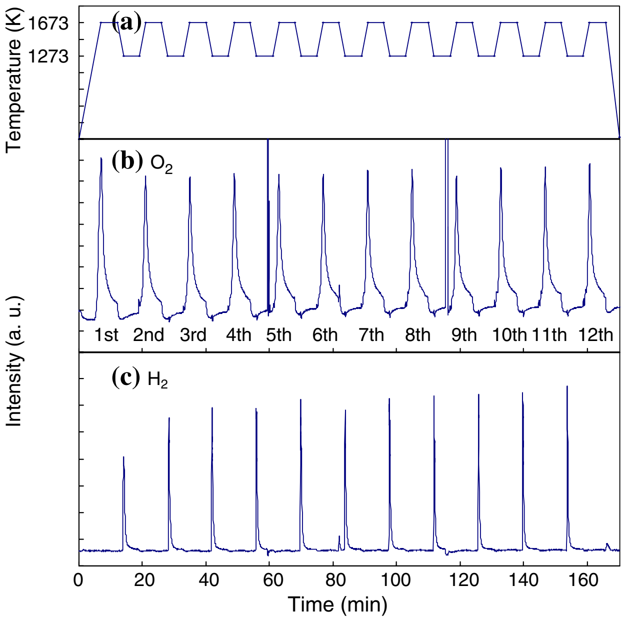

Fig. 5 Profiles of the on-line MS signal and the temperature of sample for the cyclic two-step water-splitting reaction with CeO_2–Fe_2O_3 (Ce:Fe = 8.9:1.1)

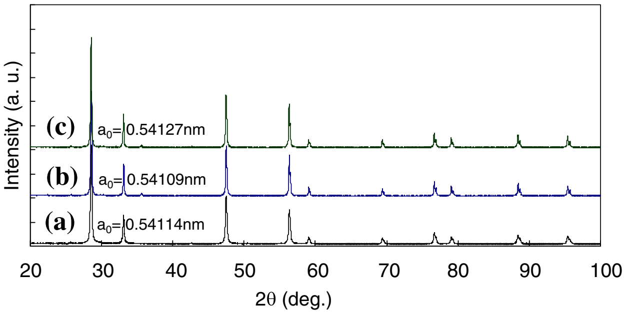

Fig. 6 XRD patterns of CeO_2–xFe_2O_3 (Ce:Fe = 8.9:1.1) with lattice constant, (**a**) starting material calcined at 823 K for 2 h, (**b**) solid product after O_2-releasing reaction and (**c**) solid product after H_2-generation reaction

the points of steam on/off because of air contamination with an exchange of the condenser in Fig. 1. The broad peak of the H_2 evolution following the 1st O_2 evolution peak was observed in the H_2-generation reaction at 1,273 K; on the other hand, the heights of H_2 evolution peaks in other runs were nearly equal. The amount of H_2 evolved in each run is approximately constant (1.9–2.0 cm^3/g). The ideal mole ratio of H_2/O_2 should equal 2 in the stoichiometric reaction; however, the average mole ratio of H_2/O_2 evolved in the 11 runs of the two-step water-splitting reaction was slightly small ($H_2/O_2 = 1.5$). This was due to the contamination of O_2 in air with a switch of valves for a change (Ar or Ar + steam) of gas passage.

The XRD spectrum of CeO_2–xFe_2O_3 with Ce:Fe = 8.9:1.1 obtained by calcining at 823 K is shown in Fig. 6a, and the spectra of the solid products after the O_2-releasing and the H_2-generation reactions are given in Fig. 6b and c, respectively, with their lattice constants. The structure of CeO_2–xFe_2O_3 solid solution was held after repetition of the two-step water-splitting reaction, since the single-phase patterns with the fluorite structure were confirmed as the starting material and the solid products after the reaction. The lattice constants of the solid products after the O_2-releasing and the H_2-generation reactions were in agreement with those of the starting material of CeO_2–xFe_2O_3 calcined at 823 K. The evaluated oxygen deficiency in the starting solid solution of CeO_2–xFe_2O_3 with Ce:Fe = 8.9:1.1 is 0.07 on the basis of the content of Fe^{3+}. The oxygen deficiencies in the solid solution of CeO_2–xFe_2O_3 produced in the O_2-releasing and the H_2-generation reactions are evaluated to be 0.1–0.15 from the contents of iron ions (Fe^{3+} and Fe^{2+}) and the amounts of O_2 gas evolved in the reaction. The increases in oxygen deficiency and cation repulsion with the two-step water-splitting reaction are small; therefore, the variation of lattice constants of CeO_2–xFe_2O_3 solid solution with the reaction is not pronounced.

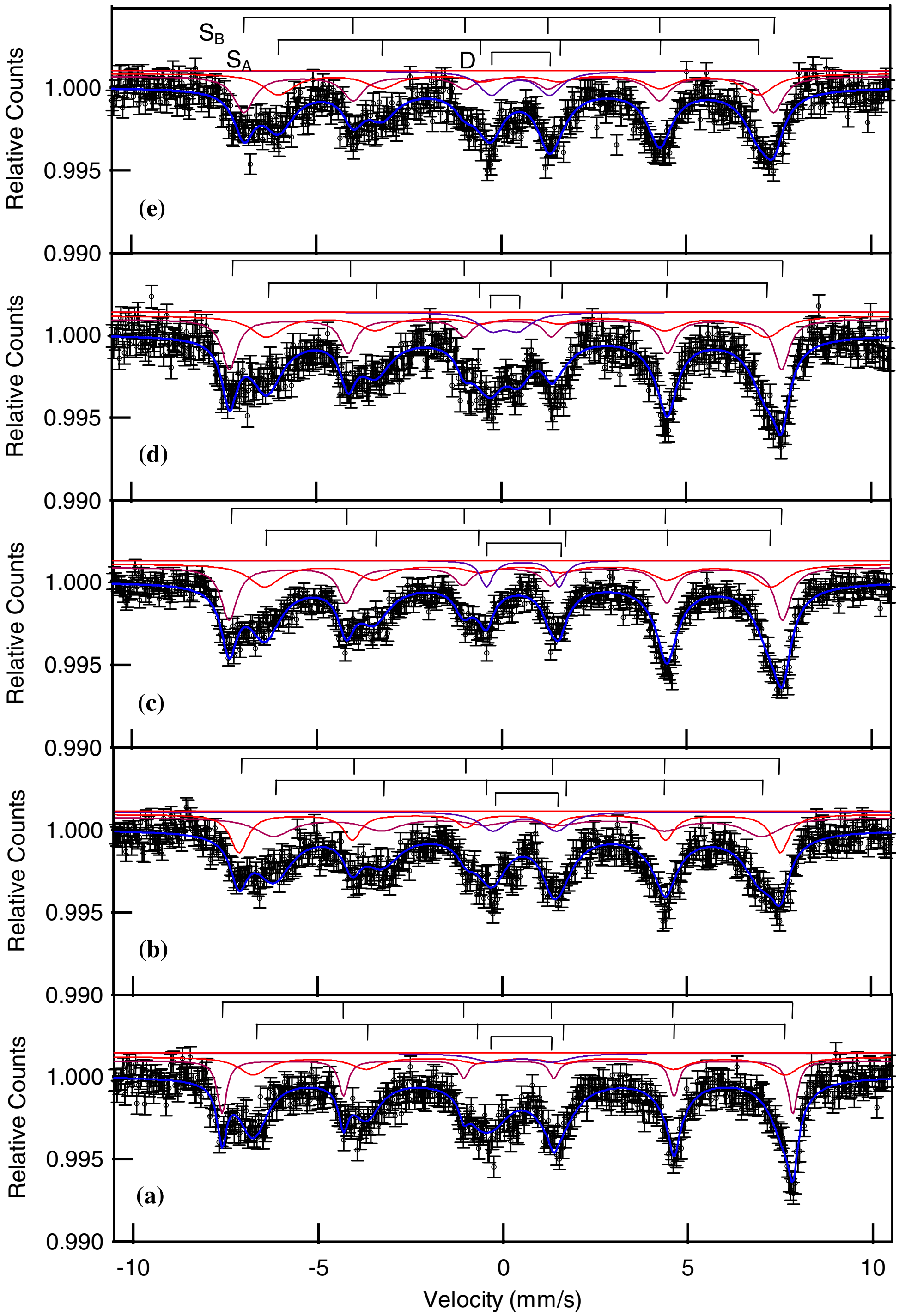

Fig. 7 Mössbauer spectra of the CeO_2–xFe_2O_3 (Ce:Fe = 8.9:1.1) after (**a**) H_2-generation reaction at 1,273 K, (**b**) O_2-releasing reaction at 1,373 K, (**c**) O_2-releasing reaction at 1,473 K, (**d**) O_2-releasing reaction at 1,573 K, and (**e**) O_2-releasing reaction at 1,673 K. D = doublet; S$_A$, S$_B$ = sextet

Mössbauer spectra of the solid products obtained by quenching in the H_2-generation reaction at 1,273 K and the O_2-releasing reaction at 1,373–1,673 K after the cyclic two-step water-splitting reaction (at the temperature of 1,273–1,673 K) with the CeO_2–xFe_2O_3 with Ce:Fe = 8.9:1.1 are shown in Fig. 7a–e, respectively. The best-fit hyperfine parameters, i.e., the isomer shift, quadrupole splitting, and the hyperfine magnetic field, are listed in Table 4. As can be seen from Fig. 7b–f, the solid products derived from the CeO_2–xFe_2O_3 solid solution in the two-step water-splitting reaction include possibly two sextets (A and B) besides a doublet. Two sets of sextets with their isomer shifts of 0.62–0.68 (mm/s) and 0.30–0.37 (mm/s) arise from valence fluctuating $Fe^{2.5+}$ between Fe^{2+} and Fe^{3+} at the octahedral sites and Fe^{3+} ions at the tetrahedral sites, respectively [14, 21]. The large peak of

Table 4 Mössbauer spectroscopy parameters for $CeO_2–xFe_2O_3$ prepared with Ce:Fe = 8.9:1.1 and reacted in the two-step water-splitting reaction

$CeO_2–xFe_2O_3$ condition		Isomer shift (mm/s)	Quadrupole splitting (mm/s)	Hyperfine magnetic field (T)
823 K calcine	D	0.35	0.98	
1,273 K	D	0.69	1.61	
H_2-generation	S_A	0.62	−0.027	44.6
	S_B	0.31	−0.038	47.9
1,373 K	D	0.80	1.73	
O_2-releasing	S_A	0.66	−0.15	41.0
	S_B	0.37	0.022	45.5
1,473 K	D	0.75	1.96	
O_2-releasing	S_A	0.65	−0.066	42.5
	S_B	0.30	−0.018	46.4
1,573 K	D	0.28	0.74	
O_2-releasing	S_A	0.64	−0.088	41.9
	S_B	0.32	−0.062	46.3
1,673 K	D	0.70	1.58	
O_2-releasing	S_A	0.68	−0.064	40.2
	S_B	0.35	0.063	44.4

D = doublet; S_A, S_B = sextet

the O_2 evolution in the 1st O_2-releasing reaction at 1,673 K corresponded to the reduction of Fe^{3+} into Fe^{2+}. In the fluorite structure, the cubic-octacoordinated Ce^{4+} is surrounded by 8 oxygen atoms; on the other hand Ce^{3+}, Fe^{3+}, and Fe^{2+} are surrounded by 6, 6, and 4 oxygen atoms with oxygen vacancies, respectively (Fig. 8a). The Fe^{3+} surrounded by 6 oxygen atoms is regarded as in tetrahedral coordination. While Fe^{2+} surrounded by 4 oxygen atoms is particularly in tetrahedral coordination, the oxygen vacancies are compensated by other neighboring O^{2-} ions in turn and the Fe^{2+} may be regarded as in tetrahedral coordination (Fig. 8b). It can be assumed that conduction of O^{2-} ions via oxygen vacancies occurs readily in the $CeO_2–xFe_2O_3$ solid solution, since the ceria-based electrolytes such as $Ce_{1-x}Ca_xO_{2-x}$ solid solution are mixed conductors with migration of O^{2-} ions via oxygen vacancies or electrons [22]. The enhanced mobility of O^{2-} ions via oxygen vacancies with the presence of Fe^{2+} and Fe^{3+} in $CeO_2–xFe_2O_3$ solid solution is presumed to promote releasing O_2 at 1,673 K and taking up oxygen from H_2O molecule at 1,273 K for $CeO_2–xFe_2O_3$. It may be concluded that the reactivity of $Ce^{4+}–Ce^{3+}$ redox system in the O_2-releasing and H_2-generation reactions with $CeO_2–xFe_2O_3$ solid solution is enhanced with the presence of Fe^{3+} and Fe^{2+} in the fluorite structure.

Fig. 8 Pathway proposed for transfer of O^{2-} and oxygen vacancy around Fe^{2+} in $CeO_2–xFe_2O_3$, (**a**) Fe^{2+} in a tetrahedral site and (**b**) Fe^{2+} in a distorted octahedral site

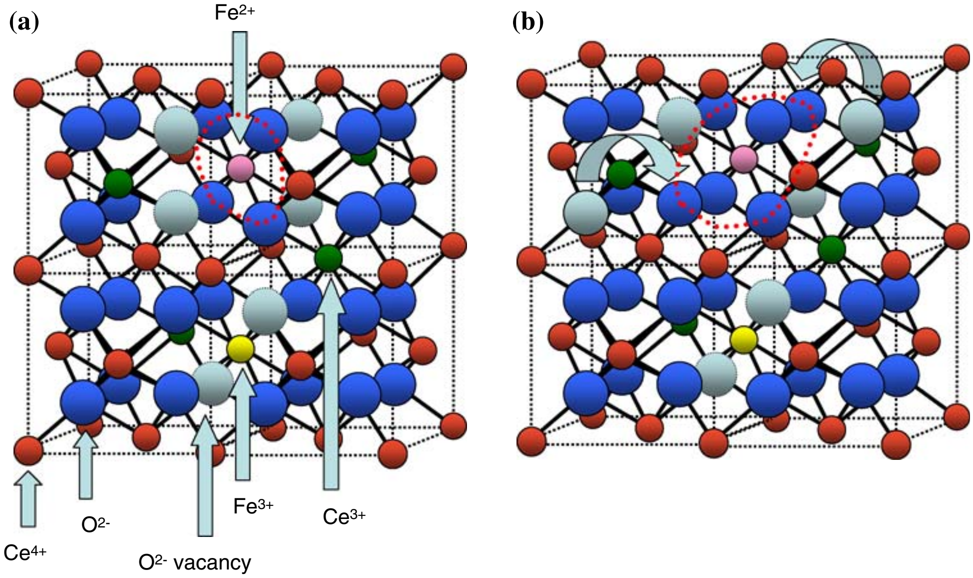

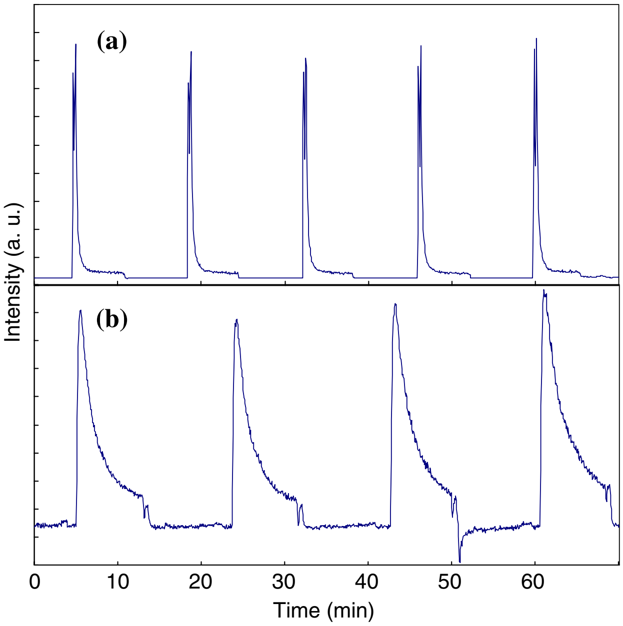

Fig. 9 Profiles of the on-line MS signal of H_2 evolution in the cyclic two-step water-splitting reaction with (**a**) CeO_2–$x$$Fe_2O_3$ (Ce:Fe = 8.9:1.1) and (**b**) $NiFe_2O_4$

H_2-generation reaction rate

Figure 9a and b show the profiles of H_2 evolution in the cyclic two-step water-splitting reaction for 70 min using CeO_2–$x$$Fe_2O_3$ with Ce:Fe = 8.9:1.1 and Ni-ferrite, respectively. The peaks of H_2-gas evolution observed in the H_2-generation reaction with CeO_2–$x$$Fe_2O_3$ were sharper than those with Ni-ferrite. The average amounts of H_2 gas evolved in 1 run of the two-step water-splitting reaction with CeO_2–$x$$Fe_2O_3$ and Ni-ferrite were 1.7 and 3.4 cm^3/g, respectively. The H_2-generation reaction rates of CeO_2–$x$$Fe_2O_3$ and Ni-ferrite were estimated to be 0.58 and 0.52 $cm^3/g{\cdot}min$, respectively. It was confirmed that the H_2-generation reaction rate of CeO_2–$x$$Fe_2O_3$ was larger than that of Ni-ferrite. The oxidation of Ce^{3+}–Ce^{4+} with steam in the fluorite structure of CeO_2–$x$$Fe_2O_3$ readily proceeds with the generation of H_2 gas in comparison with the oxidation of Fe^{2+}–Fe^{3+} in the spinel structure of Ni-ferrite. The ready oxidation of Ce^{3+}–Ce^{4+} is due to higher conductivity for O^{2-} ions via oxygen vacancies in CeO_2–$x$$Fe_2O_3$ than that in Ni-ferrite.

Conclusions

It was confirmed that Ce/Fe (Ce:Fe mole ratio) for the formation of CeO_2–$x$$Fe_2O_3$ solid solution was more than 3 (Ce:Fe = 8:2) by XRD and Mössbauer spectroscopy. The amounts of H_2 and O_2 gases evolved in the two-step water-splitting reaction with CeO_2–$x$$Fe_2O_3$ solid solutions were 0.97–1.8 and 0.60–1.1 cm^3/g, respectively; the evolved H_2:O_2 ratio was approximately equal to 2 of the stoichiometric value. These amounts of H_2 and O_2 gases were independent of the Fe content in CeO_2–$x$$Fe_2O_3$; therefore, it was suggested that the two-step water-splitting reaction with CeO_2–$x$$Fe_2O_3$ proceeded with the reduction and oxidation of Ce^{4+}–Ce^{3+} alternately. The Mössbauer spectra of CeO_2–$x$$Fe_2O_3$ supported the Ce^{4+}–Ce^{3+} redox system with the presence of Fe^{2+} and Fe^{3+} during the O_2-releasing and H_2-generation reactions. The O_2-releasing reaction at 1,673 K and H_2-generation reaction at 1,273 K with CeO_2–$x$$Fe_2O_3$ were repeated with the evolving of O_2 (1.3 cm^3/g) and H_2 (1.9 cm^3/g) gases. The large H_2-generation reaction rate was observed for the two-step water-splitting reaction with CeO_2–$x$$Fe_2O_3$ due to the Ce^{4+}/Ce^{3+} redox system. It is confirmed that CeO_2–$x$$Fe_2O_3$ is a prominent reactive ceramic for the practical solar hydrogen production.

References

1. Steinfeld A (2005) Solar Energy 78:603
2. Kodama T, Gokon N (2007) Chem Rev 107:4048
3. Abanades S, Flamant G (2006) Solar Energy 80:1611
4. Kaneko H, Miura T, Ishihara H, Taku S, Yokoyama T, Nakajima H, Tamaura Y (2007) Energy 32:656
5. Shannon RD (1976) Acta Cryst A32:751
6. Trovarelli A (1996) Catal Rev Sci Eng 38:439
7. Murray EP, Tsai T, Barnett SA (1999) Nature 400:649
8. Avgouropoulos G, Ioannides T (2003) Appl Catal A Gen 244:155
9. Jung CR, Hanb J, Namb SW, Limb T-H, Hongb S-A, Lee H-I (2004) Catal Today 93–95:183
10. Tang X, Zhang B, Li Y, Xu Y, Xin Q, Shen W (2004) Catal Today 93–95:191
11. Shan W, Feng Z, Li Z, Zhang J, Shen W, Li C (2004) J Catal 228:206
12. Kamimura Y, Sato S, Takahashi R, Sodesawa T, Akashi T (2003) Appl Catal A Gen 252:399
13. Kaneko H, Miura T, Fuse A, Ishihara H, Taku S, Fukuzumi H, Naganuma Y, Tamaura Y (2007) Energy Fuels 21:2287
14. Li G, Smith RL Jr, Inomata H (2001) J Am Chem Soc 123:11091
15. Hosokawa S, Taniguchi M, Utani K, Kanai H, Imamura S (2005) Appl Catal A Gen 289:115
16. Occelli ML, Huggins FE, Dominguez JM, Stencel JM, Gould SA (1995) Microporous Mater 4:291
17. An SY, Shim IB, Kim CS (2005) J Appl Phys 97:10Q909
18. Pérez-Alonso FJ, Granados ML, Ojeda M, Terreros P, Rojas S, Herranz T, Fierro JLG (2005) Chem Mater 17:2329
19. Pérez-Alonso FJ, Granados ML, Ojeda M, Herranz T, Rojas S, Terreros P, Fierro JLG, Gracia M, Gancedo JR (2006) J Phys Chem B 110:23870
20. Liu Q, Ma W, He R, Mu Z (2005) Catal Today 106:52
21. Taniyama T, Kitamoto Y, Yamazaki Y (2001) J Appl Phys 89:7693
22. Hurley MD, Hohnke DK (1980) J Phys Chem Solids 41:1349